Research

Cell Calcium (2001) **30**(6), 383–393

doi: 10.1054/ceca.2001.0246, available online at http://www.idealibrary.com on IDEAL®

Construction of a two-photon microscope for video-rate Ca^{2+} imaging

Q-T. Nguyen, N. Callamaras, C. Hsieh, I. Parker

Laboratory of Cellular and Molecular Neurobiology, Department of Neurobiology and Behavior, University of California, Irvine, USA

Summary We describe the construction of a video-rate two-photon laser scanning microscope, compare its performance to a similar confocal microscope, and illustrate its use for imaging local Ca^{2+} transients from cortical neurons in brain slices. Key features include the use of a Ti-sapphire femtosecond laser allowing continuous tuning over a wide (700–1000 nm) wavelength range, a resonant scanning mirror to permit frame acquisition at 30 Hz, and efficient wide-field fluorescence detection. Two-photon imaging provides compelling advantages over confocal microscopy in terms of improved imaging depth and reduced phototoxicity and photobleaching, but the high cost of commercial instruments has limited their widespread adoption. By constructing one's own system the expense is greatly reduced without sacrifice of performance, and the microscope can be more readily tailored to specific applications. © 2001 Harcourt Publishers Ltd

INTRODUCTION

The advent of confocal microscopy for imaging dynamic cellular events has revolutionized the field of intracellular Ca^{2+} signaling, particularly the study of transient, highly localized Ca^{2+} signals such as 'elementary' Ca^{2+} release events [1] and Ca^{2+} transients in individual dendritic spines [2]. A key feature of any confocal microscope used for these purposes is that it must provide good time resolution (a few tens of ms or better). Most commercial instruments are, however, designed for imaging fixed specimens, and lack the speed required to resolve intracellular Ca^{2+} dynamics. For this reason, together with the enormous cost-saving that can be accomplished by constructing one's own microscope, we had previously developed line-scan [3] and frame-scanning systems [4,5] optimized for fast intracellular Ca^{2+} imaging.

Both of those designs utilized 'conventional' confocal microscopy [6], whereby rejection of out-of-focus fluorescence was accomplished with a pin-hole aperture. A more recent method to achieve the same optical sectioning effect involves two-photon excitation of fluorophores using focused light from a femtosecond pulsed laser [7]. The extremely high instantaneous energy levels achieved when such short laser pulses are focused to a spot allows near-simultaneous absorption of two photons, each having about one-half the energy (twice the wavelength) that would normally be required for excitation. Thus, Ca^{2+} indicators such as Fluo-3 can be excited using infra-red (rather than blue) light. Furthermore, the requirement for simultaneous absorption of two photons leads to a square law relationship between intensity of the excitation light and fluorescence emission, so fluorescence excited by a femtosecond laser beam focused through a microscope objective is confined almost entirely to the focal spot. Two-photon excitation thus provides an inherent optical sectioning, so that all emitted photons (even those scattered within the specimen) provide useful information and can be collected without need for a confocal pinhole. Other advantages include greater penetration depth into scattering tissue [8], as well as reduced photobleaching and photodamage. This technique has proved to be especially useful for imaging in brain tissue [9–12].

A major factor currently limiting the widespread introduction of two-photon microscopes is their extremely high cost (typically >$500 k). Furthermore, until the recent introduction of the BioRad RTS2000 MP system, no commercial instruments were available that permitted 'real-time' frame scan imaging. To circumvent these limitations

Received 16 June 2001
Revised 27 August 2001
Accepted 27 August 2001

Correspondence to: Dr Ian Parker, Laboratory of Cellular and Molecular Neurobiology, Department of Neurobiology and Behavior, University of California, Irvine, CA 92697-4550, USA. Tel.: +1 949 824 7332; fax: +1 949 824 2447; e-mail: iparker@uci.edu

we constructed a custom video-rate two-photon system, derived from our previous design for a confocal microscope based around a resonant scanning mirror [4]. Major hardware changes include the use of a femtosecond pulsed laser for two-photon excitation, and use of wide-field fluorescence detectors. Furthermore, we developed an improved software package (applicable also to our earlier design) which captures and correctly interlaces the alternating left-right and right-left scans from the resonant *x*-scan mirror, thereby permitting acquisition to disc of full-resolution frames (500×450 pixel) at 30 fps. The total construction cost (including microscope, scan unit, computer, optical table and laser) was about $175 000; of which over $100 000 is accounted for by the femtosecond laser. We present here details of the microscope construction, characterize its performance, and illustrate applications including imaging of Ca^{2+} transients in dendrites and spines of cortical neurons.

MATERIAL AND METHODS

Microscope design

Overview

Figure 1A shows a schematic diagram of the two-photon microscope and image acquisition systems, and Figure 1B shows a photograph of the instrument with beam paths superimposed. Key components are the Ti-sapphire laser generating femtosecond pulses of IR light, the scan head, an upright Olympus BX 50 microscope, a photomultiplier detector (PMT) mounted on the microscope trinocular head, and a computer system for image acquisition and storage. In addition, the microscope is equipped with DIC optics and a CCD camera for IR DIC visualization of neurons in brain slices. The entire system (excluding computer and control electronics) is mounted on a 4×8 ft vibration-isolated optical table, using standard 0.5 in post mounts to hold beam steering mirrors and components of the scan head. The scan head is constructed on a separate 1×2 ft optical breadboard, mounted on stand-off pillars to raise the beam height so that it can be directed into the infinity space of the microscope via a dichroic mirror. A PC equipped with a linescan video acquisition card and custom software is used to construct confocal images, which can be saved directly to disc, and output as a standard RS170 video signal that can be recorded on videotape.

The following sections describe specific details of construction and use of the microscope. Further information and copies of software programs are available from the authors on request.

Laser

Excitation light for two-photon imaging is provided by a Ti-sapphire femtosecond laser (Tsunami; Spectra Physics, Mountain View, CA) pumped by a 5 W frequency-doubled Nd:YVO_4 laser (Millennia V_x; Spectra Physics). This solid-state configuration is remarkably compact, and obviates the need for dedicated water cooling and electrical supply required by the previous generation of argon ion pump lasers. Furthermore, use of a wide-band optics set allows the Tsunami to be continuously tuned over a range of about 710 to 980 nm, thus permitting flexible use of fluorophores with differing excitation spectra. We have found the laser system to be highly stable and reliable, permitting turn-key operation without user intervention except for minor alignment of external controls. In particular, the output power (about 780 mW at 780 nm with 5 W pump power) has remained consistent throughout nearly 2 year of operation, without cleaning or realignment of internal optics.

Alternative femtosecond lasers include 'single box' Ti-sapphire designs (e.g. Mai Tai, Spectra Physics). These have the advantage of a more compact laser head, and computer control of all adjustments (no mechanical knobs). Disadvantages include a somewhat lower power output and, more significantly, a narrower (100 nm) tuning range. Small, diode-pumped solid-state lasers providing femtosecond pulses are also available (e.g. CrLiSAF), but their utility is severely limited by their low power (< 50 mW) and single wavelength operation [13].

Laser safety

The beam from the Tsunami laser presents an extreme eye safety hazard: the average power is 10–100 times greater than the argon ion lasers commonly used for confocal microscopy while the pulsed beam causes retinal damage at powers about 10 times lower than a continuous beam. Moreover, depending on wavelength, the laser light appears as either a dim red or is completely invisible. For these reasons, the entire beam path is enclosed by metal housings or tubes, so there is no possibility of inadvertent exposure during normal operation. To minimize hazards during alignment of the beam into the microscope, we tune the laser down to about 730 nm (to enhance visibility), operate in CW mode, and reduce the pump laser power to a minimum.

Beam steering and diagnostics

The beam from the Tsunami laser is directed to the scan head using ultrafast protected silver mirrors (02 MFS 003; Melles Griot, Irvine, CA) to minimize pulse broadening. A small fraction of the beam is picked off by reflection from a microscope slide (not a cover slip, as this causes interference effects) and directed into a laser spectrum analyzer (Reese Instruments, Godalming, Surrey, UK). This allows measurement of the wavelength to which the laser is tuned and, by virtue of the spectral broadening that results when the laser is generating femtosecond pulses, provides

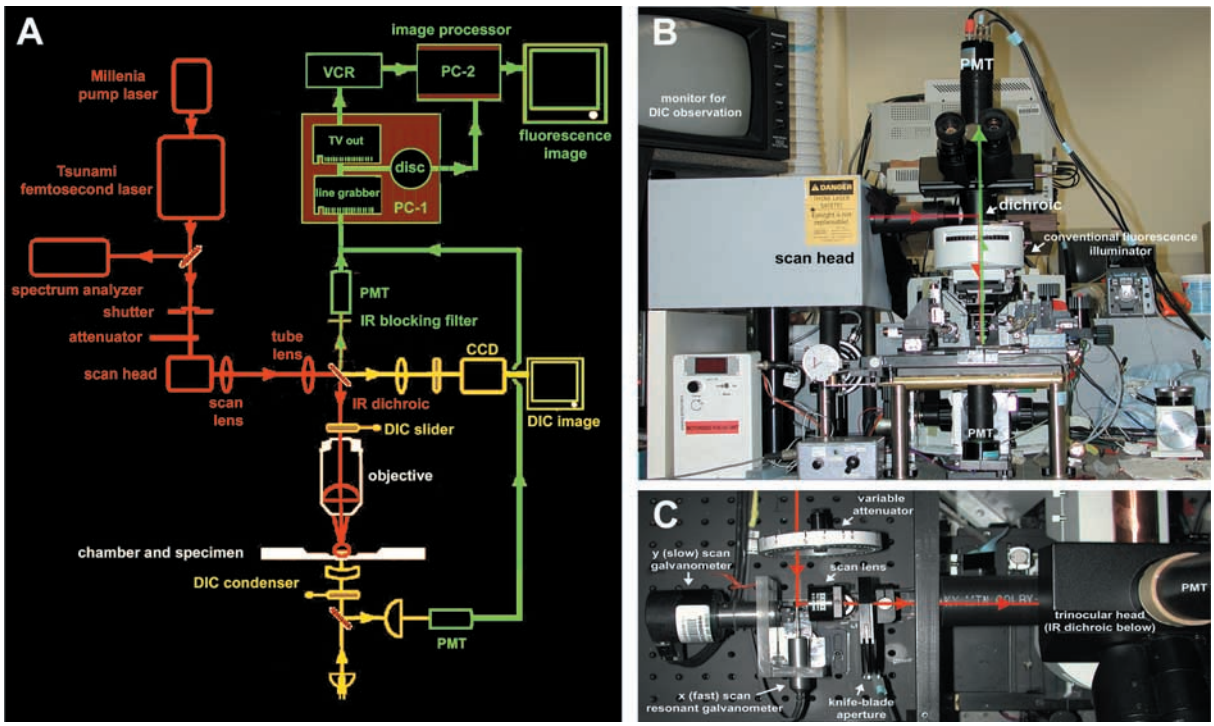

Fig. 1 (A) Overall layout of the multiphoton imaging system. Components and beam path in red represent the femtosecond laser excitation. Components in green represent the fluorescence detection pathways and image acquisition. Components in yellow represent the transmitted light DIC system for visualizing neurons during establishment of whole-cell patch. (B) Photograph of the microscope system. The laser scanner is mounted in the gray box to the left of the microscope. The locations of the upper and lower photomultiplier (PMT) detectors are indicated, together with the dichroic mirror that reflects laser light down to the objective lens. Paths of the laser beam and of emitted fluorescence light are indicated, respectively, in red and green. (C) Close-up photograph looking down on the scan head, after removing the protective cover. The path of the laser beam is indicated in red.

an indication of whether the laser is mode-locked. Laser output is measured by a power meter that can be moved into position in a narrow gap in front of the output window. An electronic shutter (Uniblitz; Vincent Associates, Rochester, NY) controls passage of the laser beam to the scan head. As noted, the entire beam path is enclosed by metal covers; but the adjusting screws for the mirror mount directing the beam into the scan head are exposed so that the beam alignment can be readily adjusted.

The duration of femtosecond light pulses is lengthened as they pass through glass elements such as microscope objectives, resulting in less efficient two-photon excitation. This pulse broadening can, in principle, be precompensated using a pair of high-index (SF-10) prisms placed in the laser beam before it enters the microscope [19,20]. However, we did not implement such a system, as our initial trials showed that it greatly complicated alignment problems while providing little improvement in image brightness.

Scan head

The scan head (Figs 1C & 2) and its associated drive electronics are essentially the same as we employed previously for constructing a one-photon video-rate confocal microscope [4]. In brief, the scan engine is comprised of two orthogonal, galvanometer-driven mirrors to allow rapid (7.9 kHz) sinusoidal scanning in the *x*-axis, and slower (30 Hz) linear scanning in the *y*-axis (Fig. 2C). These components (CRS resonant scanner, OATS scanner with off-axis paddle mirror) are available, together with associated driver circuit boards, from General Scanning Lumonics Inc. (Waterton, Mass.) Fast *x*-scanning is accomplished using the resonant scanner, which drives a small (4×6 mm), elliptical broadband-coated mirror to produce a sinusoidal change in angle. The resonant scanner vibrates at a fixed frequency (7.91 kHz: determined by its mechanical resonance), with an amplitude that is stabilized by the driver board. To minimize geometric errors arising because both mirrors cannot be placed precisely at the same telecentric plane of the microscope, the *y*-scan mirror is mounted on an off-axis paddle arm. Rotation of the *y*-galvanometer thus causes both rotation and translation of the mirror, resulting in a reduction in scanning error. Using a 10× widefield eyepiece as the scan lens, the maximum scan angles of the galvanometers provide an imaging field equivalent to approximately

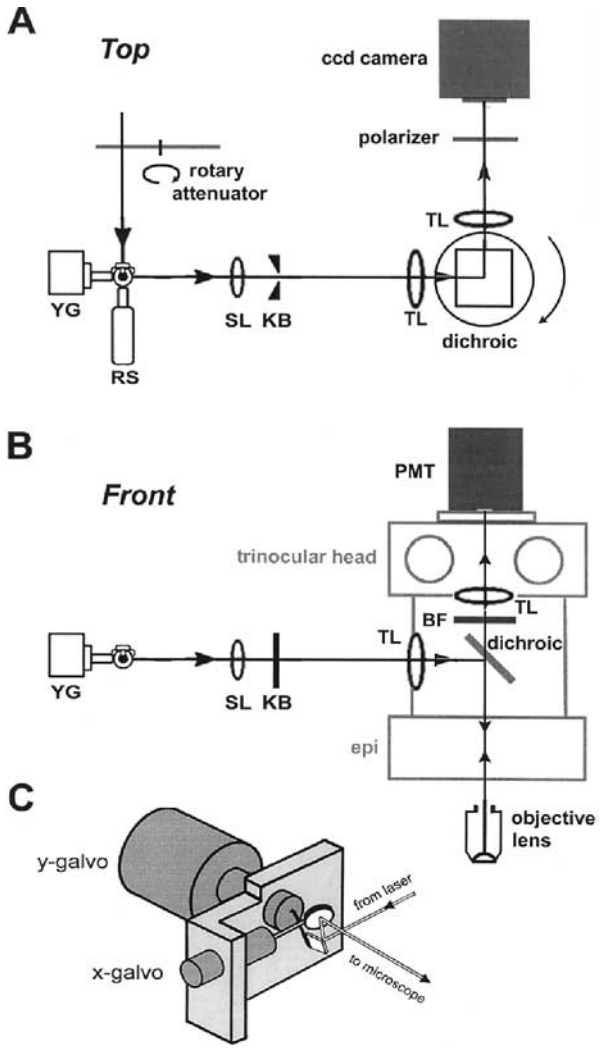

Fig. 2 (A, B) Schematic diagrams of the scan head and its coupling to the microscope viewed, respectively, from the top and front. SL = scan lens (10× widefield eyepiece); TL = tube lens; KB = variable knife-blade aperture; BF = barrier filter blocking laser light; epi = epi-fluorescence illuminator; dichroic = dichroic mirror reflecting $\lambda > 650$ nm, mounted in rotating housing. (C) Rendering of the scan head assembly.

one-third of the diameter viewed through the microscope oculars, or about 120 μm with a 40× objective lens. The scan lens is adjusted to be parafocal with the microscope oculars, and a variable knife-blade aperture located at a conjugate image plane after the scan lens allows the laser beam to be blanked off at the extremes of the sinusoidal scan where no image data are collected. The scan lens serves also as a beam expander, so that the back aperture of the objective lens is overfilled.

The scanning components are mounted on a small optical breadboard, raised on pillars so that the scanned laser beam is introduced into the infinity space created within the Olympus BX 50 microscope between the objective lens and oculars (Figs 2A & B). The laser beam is directed vertically up into the scan head via periscope mirrors, and a circular neutral density wheel (K54-081; Edmunds Industrial Optics, Barrington, NJ) allows continuously variable attenuation of the laser power from 100% to 1%. The beam from the scanner exits horizontally, and passes through a tube lens (focal length 160 mm; Olympus) to a dichroic mirror reflecting $\lambda > 675$ nm (675DCSPXR; Omega Optical, Brattleboro, VT), fitted in a custom-made, rotating adapter, mounted between the epi-fluorescence illuminator and the trinocular head of the microscope. This adapter serves a dual purpose. In one position it reflects laser light to the objective for two-photon imaging. Rotated 90° horizontally, it reflects transmitted IR light from the specimen to a CCD camera for DIC visualization. A short-pass filter ($\lambda < 650$ nm) is permanently mounted above the dichroic, and serves to block reflected and scattered laser light from reaching both the PMT detector and the oculars used for direct confocal viewing.

Detectors

With two-photon excitation, confocal sectioning is achieved without the need to pass fluorescence emission through a pinhole after descanning, which would unnecessarily impair detection efficiency. Instead, we mount a head-on prismatic face PMT (R5929 Hamamatsu Corp. Bridgewater, NJ) directly onto the camera port of the microscope trinocular head, so as to detect as much as possible of the light collected by the objective lens. The photocathode is located close to the mounting flange, and is well away from the image plane formed by the tube lens in the trinocular head, so that the image quality is not degraded by dirt on the PMT window or uneven sensitivity across the photocathode. The gain of the PMT is controlled by varying its high voltage supply (Hamamatsu C2456), and the anode current is amplified and low-pass filtered (τ about 20 ns) using the transimpedance amplifier built into the PMT socket (Hamamatsu C1053-51).

To further improve the efficiency of light detection, we added a second PMT to detect light collected through the microscope condenser. A dichroic mirror ($\lambda < 650$ nm) mounted on the microscope base below the condenser reflects light forward through a laser blocking filter and onto a side-window PMT (Hamamatsu R-928) (Figs 1A & B). The anode current is amplified and filtered as described above, and added to the signal from the 'top' PMT through a summing amplifier before connecting to the acquisition board. Using a condenser with NA = 0.9 and an objective lens of NA = 0.8 to image a slide of fluorescent pollen grains, the photon counts from both PMTs were similar. Simultaneous use of both detectors thus provides an improvement of signal-to-noise ratio at a

given laser power by a factor of about 1.4 (square root of 2), or allows the laser power to be reduced by the same factor while maintaining an equivalent image quality. Use of an oil-immersion condenser with higher numerical aperture would provide a further improvement, though the efficiency of light collection through the condenser will obviously depend upon the extent to which light is scattered and absorbed by the thickness of the specimen below the focal plane.

A difficulty with widefield detection is that the PMTs are highly susceptible to stray light. To circumvent this problem it is necessary to work in a darkened room and to surround the microscope with blackout curtains. Furthermore, sheets of black card are used to surround the area of the microscope below the stage so as to additionally shield the sub-condenser PMT.

Image acquisition

Our previous confocal scanning system [4] utilized a standard frame grabber board (DT3152; Data Translation, Malborough, MA) and software (DT-acquire) that was able to acquire image data during only the forward half of the sinusoidal *x*-scan. As a result, the frame rate was limited to 15 fps for full-frame images (500 × 450 pixels) and the specimen was exposed unnecessarily to laser light during the return scan when no data were collected. To circumvent these problems, we have now developed a stand-alone Microsoft Windows application ('e-Maging') to acquire, display and save in real-time the non-standard signals generated by the microscope. Copies of this software package are available on request to the authors, and can be utilized also in conjunction with our earlier design for a video-rate confocal microscope [4].

The e-Maging program transforms the line scans generated by the microscope into digitized video frames, and simultaneously displays and stores these image frames. Due to the sinusoidal motion of the resonant *x*-scan mirror (Fig. 3B), each complete scan consists of a forward sweep of the specimen followed by a reverse sweep as the mirror oscillates from side to side. The 'raw' image frame captured by the digitizer board thus comprises a mirror image pair of the specimen (Fig. 3A). During the dead-time required for flyback of the *y*-scan mirror following each frame scan the program reverses the order of pixels collected during the reverse sweep, and interlaces them with lines acquired during the forward scan (Fig. 3C). Finally, the resulting frame is cropped to exclude the pixels acquired during the non-linear extremes of the *x*-scan excursions, and during fly-back of the y-scan mirror (Fig. 3D). As described previously [4], deviations from linearity of the final image are within 5 pixels, despite the sinusoidal motion of the *x*-scan mirror. Images are then displayed and saved individually in picture files or sequentially as video (AVI) clips. All activities (frame acquisition, processing, display and saving) take place almost simultaneously, without dropping any frames, while leaving the user with full control of the computer. Important settings (e.g. window positions, frame grabber parameters) are saved after each session in the Windows Registry, and are automatically recalled when the program starts.

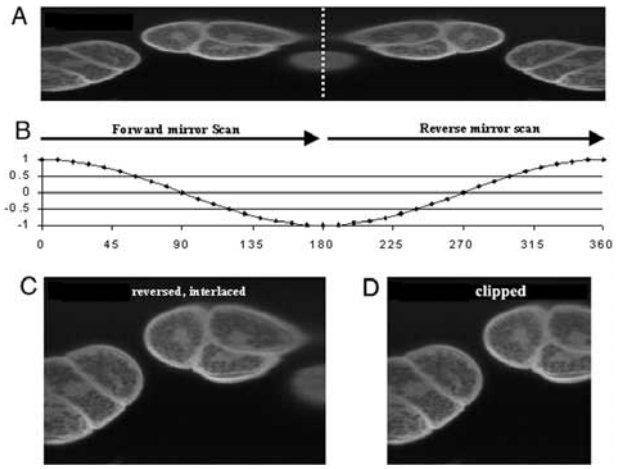

Fig. 3 Procedures for obtaining a final interlaced image using the non-linear sinusoidal resonant scan mirror. (A) The initial unprocessed image acquired by the DT-3152LS board consists of 1200 pixels × 225 lines. Each line is constructed from the forward and reverse scan of the resonant mirror, thus forming a mirror-image pair of the specimen. (B) Velocity profile of the resonant mirror as it moves forward and backward to form the image in A. (C) During the flyback time of the y-scan mirror, the computer forms an interlaced image (600 pixel × 450 line) by reversing the order of the pixels during the reverse scan, and interlacing these below the corresponding pixels in the forward scan. (D) The edges of the interlaced frame are clipped, so as to display only the central, approximately linear, portion of the sinusoidal scan.

The program was developed in Object Pascal using the Delphi 5 development environment (Borland/Inprise, Scotts Valley, CA), while time-critical code, such as pixel swapping, was written in optimized ×86 assembly language.

Acquisition hardware – E-Maging is currently being run on various Pentium II and Pentium III-based computers (>450 MHz) running Microsoft Windows 98. Frame acquisition is performed with a DT-3152LS PCI frame grabber (Data Translation, Malborough, MA) operating in line-scan mode. Required connections comprise the luminance signal from the PMT, the line sync and the frame sync. Pixel sampling frequency is usually set to 15 MHz by the internal clock of the DT3152-LS. The board digitizes the analog signal from the PMT with a resolution of 8 bits.

User interface – The program displays a video window displaying incoming, processed image frames, and

a second window with controls for acquisition. Pull-down menus allow the user to configure parameters such as the settings of the DT3152-LS, or the dimensions of the image. The program automatically calculates the frame rate from the size of the frame, and the screen resolution can be changed to accommodate a particular frame size. The live image is shown in the main window, either in pseudo color (where the lowest level is dark blue and the highest level is red) or in gray scale. For maximum speed, the Windows display is set to 256 colors, and the frame grabber is programmed to re-map the 256 possible values for each pixel into 236 levels, thereby excluding the 20 colors used by Windows. Rapid frame display is achieved utilizing the DirectDraw technology included in the DirectX 7 extension to Windows.

Saving data to disk – Image streaming can be done in two modes: continuous or single-sweep. In continuous mode, a pre-set number of frames are saved to disk. This mode requires a computer able to achieve sustained data transfer to disk at about $6\,MB\,s^{-1}$. Alternatively, single-sweep recording saves a pre-set number of frames to memory in real-time, which are subsequently transferred to disc. Data files use the AVI (Audio Video Interleaved) file format to store pseudocolor or gray scale, uncompressed frames. This widely-used format provides real time video streaming with the capability of combining, in the same file, data streams such as electrophysiological recordings. Furthermore, video clips can be readily reviewed using the Windows Media Viewer. Data file names are automatically allocated by e-Maging, and are incremented for each new file.

As well as capturing image sequences as AVI files, individual frames can be captured in 'snapshot' mode as bitmap (BMP) files. Snapshot images can be a single frame, or an average of any pre-set number of frames. Both streaming and snapshot modes can be triggered manually, or via a TTL input.

Export to Metamorph – We use the Metamorph package (Universal Imaging, WestChester, PA) for image processing and analysis. However, Metamorph cannot read AVI files, but instead uses a proprietary stack (STK) format. We therefore developed a utility (AVItoSTK) to convert AVI files into stack files. Conversion is fast, taking $<5\,s$ for a (60 MB) AVI file. Alternatively, a graphics card providing a standard composite video output is used to send an analog signal of the live screen display to a video digitizer card in a second computer running Metamorph [4]. This results in a slight degradation of image quality, but has advantages in that Metamorph can then be used to control image acquisition for purposes such as multi-dimensional imaging.

RESULTS

In this section we describe tests of the microscope resolution, and illustrate applications of two-photon microscopy for imaging cellular structure as well as dynamic calcium transients. Furthermore, we compare the performance of the two-photon video-rate microscope with that of the similar one-photon microscope we had previously described [4]. Unless otherwise noted, all two-photon images were obtained using excitation at 780 nm (ca. 80 fs pulse duration at the laser), with emission at <650 nm. Objective lenses (Olympus, infinity corrected) included: 40×, NA 0.8, IR, water immersion; 60×, NA 1.2 water immersion (corrected for 170 μm cover-glass); 40×, NA 1.35, oil immersion).

Spatial resolution

Figures 4A & B shows two-photon images of fluorescent beads, illustrating the limiting lateral and axial resolutions obtained using an objective lens with high numerical aperture (60× water immersion, NA 1.2). A convenient measure of the spatial resolution is provided by the point spread function, which was determined as the full-width at half-maximal intensity (FWHM) of fluorescence imaged from sub-resolution beads. Using 100 nm diameter beads, adhered to a cover glass and imaged in water, we obtained lateral and axial FWHM values of about 350 and 900 nm, respectively. These values may be compared to measurements under similar conditions with one-photon excitation (300 nm lateral and 800 nm axial) [4].

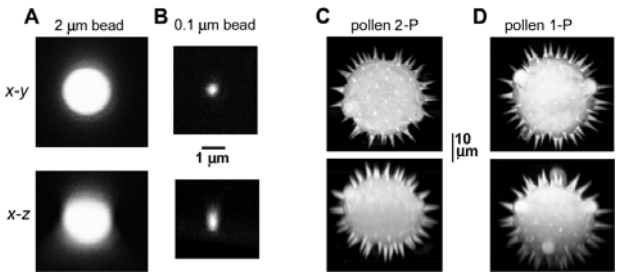

Fig. 4 Lateral and axial resolution tests. All images show maximum value projections derived from image stacks (average of 30 video frames for each plane) obtained at axial spacings of 0.25 μm (A,B: obtained using a 60× water immersion objective with NA = 1.2) or 0.5 μm (C,D: 40× oil immersion objective, NA = 1.35). The upper row shows *x-y* images (i.e. 'top' view), and the lower row *x-z* images ('side' view). (A) Lateral and axial views of a 2 μm diameter fluorescent bead (fluosphere: Molecular Probes). (B) Corresponding images of a 0.1 μm diameter bead, showing the point-spread function of the microscope. (C) Images of a 'spiky' fluorescent pollen grain (mixed pollen grain slide: Carolina Biological Supply) obtained with two-photon excitation. (D) Corresponding images of a similar pollen grain obtained using a one-photon video-rate microscope (488 nm excitation; >510 nm emission) equipped with the same objective lens.

Thus, the spatial resolution of two-photon microscopy is better than might be expected from the use of IR excitation with wavelengths nearly double that employed for conventional confocal microscopy, probably because the quadratic dependence of fluorescence excitation ensures that the signal arises largely from the center of the diffraction-limited laser spot.

A further comparison of spatial resolution is provided in Figures 4C & D, illustrating, respectively, two-photon and one-photon images of 'spiky' pollen grains: a readily available specimen that provides a good test of the ability of a confocal microscope to section through protruding spines while rejecting out-of-focus fluorescence from the body of the pollen grain. Both the lateral (upper) and axial (lower) resolutions were closely similar with both imaging modalities; but the decline in image brightness with increasing distance through the pollen grain was substantially reduced with two-photon excitation.

Imaging depth

A major advantage of two-photon microscopy is the ability of this technique to image more deeply into a specimen than is possible with conventional confocal microscopy. This arises from at least three factors: (1) The IR excitation light is scattered less than shorter wavelengths (2) excitation occurs only at the focal spot, and IR light passes through the rest of the specimen without being absorbed by the fluorophore, and (3) scattering of emitted fluorescence light does not blur the image, but instead contributes to the image brightness. The superior ability of two-photon excitation for imaging deeply into specimens is illustrated in Figure 5; again comparing one-photon and two-photon versions of our video-rate confocal scanner.

Figure 5A first demonstrates the need to use an appropriately matched objective lens, whether using single- or two-photon modalities. The traces show the average fluorescence intensity measured while focusing the microscope at different depths into an aqueous solution of fluoresceine beneath a cover glass. Using an oil-immersion objective, the fluorescence monitored by conventional confocal microscopy declined steeply with increasing depth into the solution; falling to one-half within 15 μm of the cover glass, owing to spherical aberration resulting from the refractive index mismatch between the immersion oil and water. Substituting a water-immersion objective with similar NA resulted in a dramatic improvement; with a half-decline in fluorescence at about 80 μm. A further improvement was then obtained using two-photon excitation through the same objective, such that the fluorescence declined by as little as 10% at a depth of 100 μm.

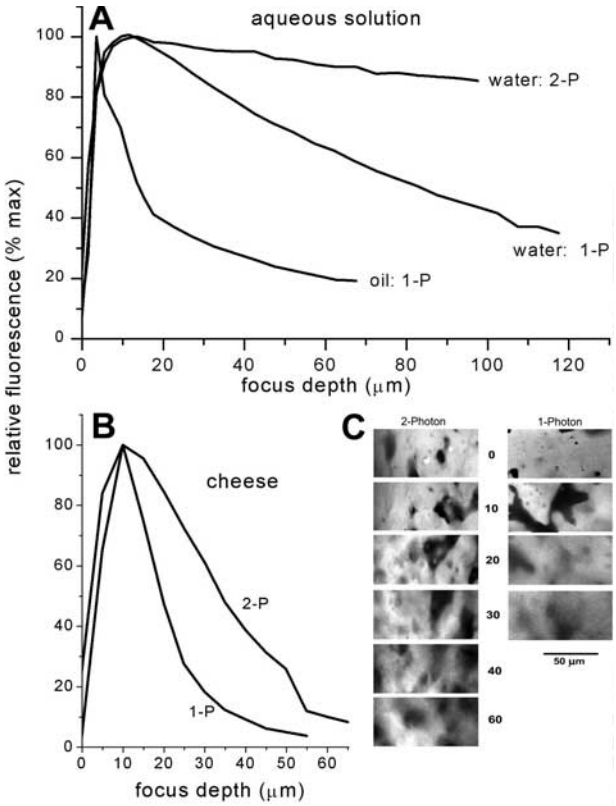

Fig. 5 Comparison of imaging depth using single- and two-photon excitation. (A) Normalized fluorescence detected when focusing at different depths into an aqueous solution of 50 μM fluoresceine. Measurements were obtained from a thick (ca. 500 μm) film of solution sandwiched below a cover glass, and the traces illustrate results obtained using an oil immersion objective (40×, NA = 1.35) with one-photon (488 nm) excitation, a water immersion objective (60×, NA = 1.2) with one-photon excitation (488 nm), and the same water immersion objective with two-photon excitation (780 nm). (B) Similar measurements obtained in a scattering medium using the water immersion objective with one- and two-photon excitation. The specimen was a slice (1 mm) of cheddar cheese, that had been soaked for 2 h in an aqueous solution of 50 μM fluoresceine, and was imaged through a cover glass. Measurements show normalized fluorescence averaged over the 50 × 50 μm scan area. (C) Sample images obtained at different depths (indicated in μm) into the cheese, illustrating the ability of two-photon imaging to resolve detail at greater distances into a highly scattering specimen. Each image is individually contrast enhanced.

To compare the imaging capabilities of 1- and two-photon microscopy in a highly scattering specimen, we stained a block of cheese (Cheddar) with fluoresceine. The fluorescence obtained with two-photon excitation declined much less steeply with increasing depth into the specimen than with one-photon confocal imaging (Fig. 5B). Furthermore, this fall-off in two-photon signal could be partly compensated by increasing the laser power, allowing useful resolution of structure to depths at least twice as great as could be achieved by conventional confocal imaging (Fig. 5C).

Limitations on signal brightness

Video-rate imaging permits detection of relatively few photons during the brief (*66* ns) dwell time at each pixel. Statistical fluctuations in photon count, therefore, set a severe limit on the signal-to-noise ratio that can be achieved. One way to improve the signal brightness is simply to increase the laser power incident on the specimen. A concern then is whether the fluorophore may saturate at high intensities. In practice this appears not to be a limitation. For example, fluorescence of cells expressing a red fluorescent protein (DsRed; excited at 950 nm) increased following the expected quadratic relationship with laser intensity up to the point where all attenuation in the laser path was removed (power at the specimen about 80 mW). Satisfactory imaging of bright specimens (e.g. fluorescent pollen grains, cells expressing GFP) could be achieved using an average laser power at the specimen of about 5 mW, whereas imaging neurons loaded with calcium indicator typically required >15 mW.

A more important restriction when imaging live cells is set by the onset of photodamage. In cortical neurons filled with a calcium indicator (Calcium green-1 or Oregon Green-1) this was apparent as an increase in resting fluorescence, accompanied by a decreased resting potential and input resistance. Photodamage could be reduced by minimizing the time for which a cell was exposed to the laser, and by decreasing the laser intensity. The relationship between photodamage and laser intensity appeared to be even steeper than the quadratic relationship for fluorescence excitation. Efforts to improve recordings by increasing the laser intensity thus rapidly reached a region of diminishing returns, where the shortened time available for imaging before onset of damage more than obviated any increase in fluorescence brightness. Recent quantitative studies of photodamage by femtosecond laser pulses [16,17] indicate that this probably results through 3-photon excitation of endogenous cellular constituents. Hopt and Neher [16] suggest, therefore, that improvements may be possible by deliberately lengthening the pulse width, and by underilluminating the back aperture of the objective so as to degrade axial resolution and thereby extend the focal volume excited within sufficiently thick fluorescent specimens: procedures that are both the opposite of commonly held wisdom.

Overall, the fluorescence signals we obtained using two-photon excitation of fluorophores including Fluo-3, Oregon Green, GFP variants and DsRed were appreciably dimmer than obtained by conventional confocal microscopy, even when the pinhole of the confocal microscope was stopped down to provide optimal spatial resolution [18]. Our system is, therefore, designed to optimize the collection and detect of emitted photons. Collection efficiency is enhanced by use of high-aperture objectives and use of a wide-field detector placed close to the objective, while collection of light through the condenser offers a further modest improvement. The detection efficiency of photomultipliers is, unfortunately, rather poor (quantum efficiency $<20\%$ at 530 nm, and decreasing at longer wavelengths). However, photomultipliers have other advantages – including large detector area, linear response at high photon flux ($>10^9$ photons s^{-1} in analog mode) and low dark count – that make them the only practicable detector type for this application. Although avalanche photodiodes provide a much better quantum efficiency ($>60\%$), they become highly non-linear at count rates above a few MHz, corresponding to an average of <0.1 photon per pixel when scanning at video rate.

Direct-view two-photon imaging

The optical sectioning effect of conventional (one-photon) confocal microscopes is achieved by passing the de-scanned fluorescence emission beam through an aperture so as to reject out-of-focus fluorescence. Except in the special case of systems where the aperture is physically scanned across the specimen (e.g. Nipkow disc designs), it is not, therefore, possible to directly view a confocal image by eye; but rather the image must be reconstructed by a computer. This limitation does not apply to two-photon imaging, where the optical section is achieved because fluorescence is excited only at the focal spot. Furthermore, the rapid scan rate (30 fps) of the present system allows a virtually flicker-free, true-color confocal image to be viewed through the microscope oculars. By mounting a film or digital camera on the microscope in place of the photomultiplier it is, therefore, possible to obtain confocal true-color photographs (Fig. 6B) that are much sharper than is possible by conventional epifluorescence excitation (Fig. 6C).

Calcium signals in dendrites and spines

Figure 7 illustrates the use of two-photon microscopy to image calcium signals from local regions of neuronal dendrites and synaptic spines in living brain slices. Experiments were done using cortical slices prepared from P12-P20 mice, and dendrites were imaged about 80 μm below the surface of the slice. Pyramidal neurons were loaded by equilibration (about 30 min) from a whole-cell patch pipette filled with intracellular solution including 100 μM Oregon green BAPTA-1 (OG-1), and were visualized through a 40× water immersion objective (NA = 0.8) using two-photon excitation at 780 nm. Figure 7A shows the ability of the microscope to resolve

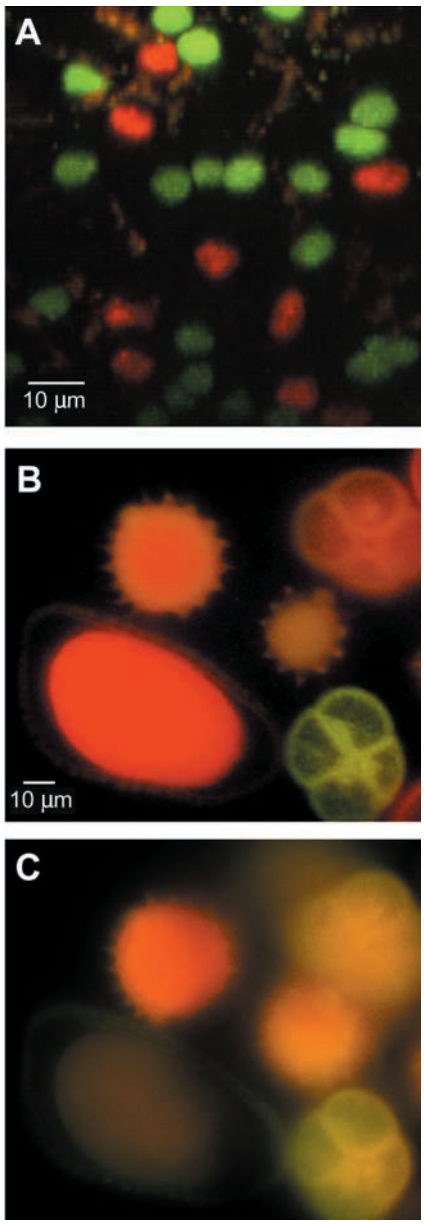

Fig. 6 Multi-color and direct-view two-photon imaging. (A) An *x-z* ('side') image of a mouse lymph node showing T-cells (green; stained with CFSE) and B-cells (red; stained with CMTMR). The image was reconstructed from a stack of *x-y* two-photon images at 0.5 µm increments, using a computer controlled filter wheel to acquire paired images at each plane at wavelengths of 510–550 nm and 600–650 nm. (B) Direct-view two-photon imaging. Fluorescent pollen grains were excited by the scanned femtosecond laser beam (780 nm), and photographed by a color digital camera (Nikon Coolpix 990) mounted on the trinocular photoport of the microscope. (C) The same pollen grains photographed by conventional (one-photon) epi-fluorescence excitation.

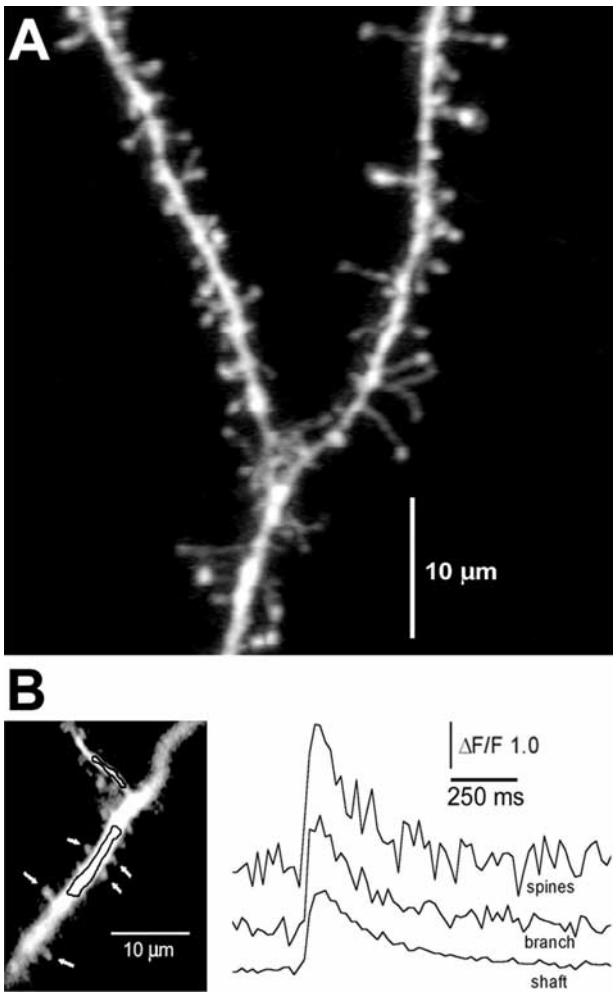

Fig. 7 Calcium imaging in a brain slice. (A) Two-photon image showing synaptic spines on the dendrites of a cortical pyramidal neuron loaded with Oregon Green 488 BAPTA 1. The image is a maximum value projection derived from a stack (average of 30 frames at each plane) acquired at 0.5 µm intervals. (B) Calcium signals in dendrites and spines of a cortical pyramidal neuron evoked by action potentials. Image at the left is an average of 80 frames at a single plane. Measurements of fluorescence were obtained from the main dendritic shaft, a fine side branch (regions of interest marked by black outlines), and from selected spines (arrows). The traces show averaged fluorescence signals from these regions in response to stimulation by injection of a 200 ms depolarizing current pulse into the cell soma, which triggered a burst of 3–4 action potentials. Each trace is an average from eight successive stimuli at 10 s intervals, and signals from the five indicated spines were further averaged together.

synaptic spines and processes, and was obtained by imaging the resting fluorescence of OG-1 at 0.5 µm sections into the slice. Figure 7B further illustrates dynamic Ca^{2+} signals recorded from small regions of dendrites, and from synaptic spines, in response to stimulation by antidromic action potentials.

DISCUSSION

The paper describes the construction of a video-rate two-photon microscope, and its application for imaging local

Ca^{2+} transients in neurons. Several other groups have constructed two-photon microscopes, either by building scanning systems from scratch or by modifying commercial confocal scanners [13–15,18–20]. However, there is only one report describing construction of a video-rate two-photon system, and that was based on modification of a now-discontinued commercial instrument [21].

Our primary motivation for undertaking construction of a two-photon microscope was economic; a complete two-photon imaging system can be constructed for a component cost of about one-third that the only commercial product offering video-rate two-photon imaging (BioRad RTS2000 MP). Moreover, the system can be more easily adapted for specific tasks, and there is no need for a service contract as the investigator becomes well qualified to undertake maintenance. Nevertheless, the cost of even a custom-built two-photon system is considerable (principally because femtosecond lasers remain expensive), and is about four times greater than for construction of an equivalent one-photon confocal system. It is, therefore, reasonable to ask whether the advantages of two-photon imaging justify the expense – are two photons really better than one?

Strong points include the increased depth to which it is possible to image into thick, scattering specimens; the restriction of photobleaching to the focal pane being imaged; and the possibility to excite multiple fluorophores by virtue of their generally broad two-photon excitation spectra [22]. Two-photon excitation also minimizes phototoxicity during long-term imaging [23], although observations of highly non-linear photodamage processes [16,17] indicate that careful selection of laser wavelength and power is necessary to achieve benign imaging conditions. A major disadvantage is that fluorescence signals are generally dimmer with multi- rather than single-photon excitation. This problem is further exacerbated by the brief pixel dwell time available for integration of photon counts when imaging at video rate, and requires an optical system designed to maximize light collection.

Our overall experience is that two-photon imaging is not a panacea [24], but that it does provide compelling advantages over confocal microscopy for certain specific applications – most notably the imaging of live cells in thick tissues and organs. The use of video-rate scanning further extends the utility of this technique to the study of fast dynamic processes. For example, we are presently using the system described here to study calcium signals in neuronal dendrites and for imaging the motility of lymphocytes within intact lymph nodes. The complexity of femtosecond lasers has previously presented a barrier to the adoption of two-photon microscopy, but the present generation of modelocked Ti-sapphire lasers function as virtually 'turnkey' devices which can be used by biologists without special laser expertise. The high price of commercial two-photon microscopes then remains the major factor limiting their more widespread use. By constructing one's own instrument the cost can be reduced to a level that is more easily justified by an individual investigator. Moreover, the microscope can be readily tailored for specific applications and, as we have emphasized before [4,5], the task of constructing a laser-scan microscope is less daunting than one might think.

ACKNOWLEDGEMENTS

We thank Dr G. Stutzmann for help with brain slice experiments, Dr M. Miller for help with lymphocyte imaging, and Dr J. Kahle for editorial assistance. This work was supported by grant GM48071 from the NIH.

REFERENCES

1. Parker I, Choi J, Yao Y. Elementary events of InsP3-induced Ca^{2+} liberation in Xenopus oocytes: hot spots, puffs and blips. *Cell Calcium* 1995; **20**: 105–121.
2. Eilers J. Fast confocal fluorescence imaging of subcellular calcium dynamics. In: R. Yuste, F. Lanni, A. Konnerth (eds). *Imaging neurons*. Cold Spring Harbor Laboratory Press, 2000, pp 15.1–15.10.
3. Parker I, Callamaras N, Wier WG. A high-resolution, confocal laser-scanning microscope and flash photolysis system for physiological studies. *Cell Calcium* 1997; **21**: 441–452.
4. Callamaras N, Parker I. Construction of a confocal microscope for real-time x-y and x-z imaging. *Cell Calcium* 1999; **26**: 271–279.
5. Sanderson MJ, Parker I. Video-rate confocal microscopy. *Meth Enzymol* 2002 (in press).
6. Pawley J.B. *Handbook of Biological Confocal Microscopy*, 2nd Edition. Plenum Press, New York.
7. Denk W, Strickler JH, Webb WW. Two-photon laser scanning fluorescence microscopy. *Science* 1990; **248**: 73–76.
8. Centonze VE, White JG. Multiphoton excitation provides optical sections from deeper within scattering specimens than confocal imaging. *Biophys J* 1998 **75**: 2015–2024.
9. Denk W, Sugimori M, Llinas R. Two types of calcium response limited to single spines in cerebellar Purkinje cells. *Proc Natl Acad Sci USA* 1995; **92**: 8279–8282.
10. Yuste R, Denk W. Dendritic spines as basic functional units of neuronal integration. *Nature* 1995; **375**: 682–684.
11. Svboda K, Helmchen F, Denk W, Tank W. Spread of dendritic excitation in layer 2/3 pyramidal neurons in rat barrel cortex in vivo. *Nat Neurosci* 1999; **2**: 65–73.
12. Koester HJ, Sakmann B. Calcium dynamics in single spines during coincident pre- and post-synaptic activity depend on relative timing of back-propagating action potentials and subthreshold excitatory postsynaptic potentials. *Proc Natl Acad Sci USA* 1998; **95**: 9596–9601.
13. Majewska A, Yiu G, Yuste R. A custom-made two-photon microscope and deconvolution system. *Pflugers Arch – Eur J Physiol* 2000; **441**: 398–408.
14. Soeller C, Cannell MB. Construction of a two-photon microscope and optimization of illumination pulse duration. *Pflugers Arch* 1996; **432**: 555–561.

15. Wier WG, Balke CW, Michael JA, Mauban JR. A custom confocal and two-photon digital laser scanning microscope. *Am J Physiol* 2000; **278**: H2150–H2156.
16. Hopt A, Neher E. Highly non-linear photodamage in two-photon fluorescence microscopy. *Biophys J* 1999; **80**: 2029–2036.
17. Koester HJ, Baur D, Uhl R, Hell SW. Ca^{2+} fluorescence imaging with pico- and femtosecond two-photon excitation: signal and photodamage. *Biophys J* 1999; **77**: 2226–2236.
18. Tan YP, Llano I, Hopt A, Wurriehausen F, Neher E. Fast scanning and efficient photodetection in a simple two-photon microscope. *J Neurosci Meth* 1999; 92: 123–135.
19. Potter SM. Two-photon microscopy for 4D imaging of living neurons. In: R. Yuste, F. Lanni, A. Konnerth (eds). *Imaging neurons*. Cold Spring Harbor Laboratory Press. 2000, pp 20.1–20.16.
20. Diaspro A, Corosu M, Ramoino P, Robello M. Adapting a compact confocal microscope system to a two-photon excitation fluorescence imaging architecture. *Microsc Res Tech* 1999; **47**: 196–205.
21. Fan GY, Fujisaki H, Miyawaki A, Tsay R-K, Tsien RY, Ellisman MH. Video-rate scanning two-photon excitation fluorescence microscopy and ratio imaging with cameleons. *Biophys J* 1999; **76**: 2412–2420.
22. Xu C. Two-photon cross sections of indicators. In: R. Yuste, F. Lanni, A. Konnerth (eds). *Imaging neurons*. Cold Spring Harbor Laboratory Press. 2000, pp 19.1–19.9
23. Mohler WA, Squirrell JM. Multiphoton imaging of embryonic development. In: R. Yuste, F. Lanni, A. Konnerth (eds). *Imaging neurons*. Cold Spring Harbor Laboratory Press. 2000, pp 21.1–21.11.
24. Potter SM. Vital imaging: two photons are better than one. *Curr Biol* 1996; **6**: 1595–8.